Published in final edited form as:
J Neuroimmune Pharmacol. 2011 September ; 6(3): 330–340. doi:10.1007/s11481-010-9236-5.

Neuronal PINCH is Regulated by TNF-α and is Required for Neurite Extension

Asavari Jatiani,
Department of Neuroscience, Temple University School of Medicine, 3500 N. Broad St., MERB 750, Philadelphia, PA, USA

Paola Pannizzo,
Department of Neuroscience, Temple University School of Medicine, 3500 N. Broad St., MERB 750, Philadelphia, PA, USA

Elisa Gualco,
Department of Oncology, Biology and Genetics, University of Genoa, Genoa, Italy

Luis Del-Valle, and
Department of Pathology, Louisiana State University, New Orleans, LA, USA

Dianne Langford
Department of Neuroscience, Temple University School of Medicine, 3500 N. Broad St., MERB 750, Philadelphia, PA, USA, tdl@temple.edu

Abstract

During HIV infection of the CNS, neurons are damaged by viral proteins, such as Tat and gp120, or by inflammatory factors, such as TNF-α, that are released from infected and/or activated glial cells. Host responses to this damage may include the induction of survival or repair mechanisms. In this context, previous studies report robust expression of a protein called particularly interesting new cysteine histidine-rich protein (PINCH), in the neurons of HIV patients' brains, compared with nearly undetectable levels in HIV-negative individuals (Rearden et al., J Neurosci Res 86:2535–2542, 2008), suggesting PINCH's involvement in neuronal signaling during HIV infection of the brain. To address potential triggers for PINCH induction in HIV patients' brains, an in vitro system mimicking some aspects of HIV infection of the CNS was utilized. We investigated neuronal PINCH expression, subcellular distribution, and biological consequences of PINCH sequestration upon challenge with Tat, gp120, and TNF-α. Our results indicate that in neurons, TNF-α stimulation increases PINCH expression and changes its subcellular localization. Furthermore, PINCH mobility is required to maintain neurite extension upon challenge with TNF-α. PINCH may function as a neuron-specific host-mediated response to challenge by HIV-related factors in the CNS.

Keywords

HIV; CNS; Neuron; TNF-α

Correspondence to: Dianne Langford.

Introduction

HIV enters the CNS early after initial infection and at various times throughout the disease resulting in multiple insults on cells of the brain. Synaptodendritic damage to neurons can occur either directly by viral proteins or indirectly by inflammatory factors released from infected/activated glial cells. Viral proteins such as Tat and gp120, and host inflammatory factors including TNF-α, are among those responsible for neuronal dysfunction and synaptodendritic disturbances in HIV (Bansal et al. 2000; Buscemi et al. 2007; Kim et al. 2008; Yao et al. 2009). However, disruptions in synaptodendritic communication and decreased network complexity have been shown to be at least partially reversible (for review, see Ellis et al. 2007), suggesting the induction of host-mediated repair mechanisms.

In this context, our previous studies reported robust expression of particularly interesting new cysteine histidine-rich protein (PINCH) in the brains and CSF of HIV patients, compared with nearly undetectable levels in HIV-negative individuals (Rearden et al. 2008). Our results strongly suggested PINCH's involvement with neuronal signaling during HIV infection of the brain. Other studies reported increased PINCH expression and aberrant localization patterns in post-injury Schwann cells and dorsal root ganglia neurons in the peripheral nervous system, suggesting a role in repair after neuronal damage and myelin loss (Campana et al. 2003).

PINCH is a highly conserved intracellular protein that consists of five LIM domains and a short C-terminal tail (Rearden 1994; Wu 2004). Although PINCH does not have a catalytic domain, it provides a framework for bidirectional signal transduction between the extracellular matrix and the intracellular network (Wu 1999). A main role of PINCH is to guide integrin-linked kinase (ILK) to focal adhesions, which in turn form important points of communication with the extracellular matrix. The LIM1 domain of PINCH binds to the first ankyrin-repeat of ILK's N-terminus and is required for ILK localization to focal adhesions, as mutagenesis of LIM1 prevents binding to ILK and ILK's localization to focal adhesions (Li et al. 1999). During development, the PINCH–ILK complex regulates cell–matrix and cell–cell adhesions, and maintains cell polarity and survival (Li et al. 2005). Studies addressing neuronal polarization indicate that PINCH–ILK interactions are key in maintaining axon-dendrite polarity (Guo et al. 2007). The LIM4 domain of PINCH interacts with Nck-2, a Src homologue adaptor protein, to regulate several key components of growth factor-mediated kinase signaling through the MAPK-p38 cascade to promote neurite outgrowth (Tu et al. 1998).

To address potential triggers for PINCH induction in HIV patients' brains, an in vitro system mimicking some aspects in the CNS during HIV infection was utilized. We investigated neuronal PINCH expression, subcellular distribution, and biological consequences of PINCH sequestration upon challenge with Tat, gp120, and TNF-α. These studies indicate that not only is PINCH increased upon stimulation with TNF-α but it must also be free to migrate throughout the cell to maintain neurite extensions.

Methods and materials

Tissue acquisition and neuropathological examination

Frontal cortex brain tissue was provided by the HIV Neurobehavioral Research Center, California NeuroAIDS Tissue Network, UCSD, San Diego, CA, USA. Temple University Office for Human Subjects Protections approved all studies conducted. The diagnosis of HIVE was based on criteria established by the American Academy of Neurology and the HIV Neurobehavioral Research Center group as previously described (Langford et al. 2004b; Del Valle and Pina-Oviedo 2006; Cherner et al. 2007). Briefly, HIVE diagnoses

included areas of myelin pallor, perivascular cuffs of mononuclear inflammatory cells, multinucleated giant cells, microglial nodules, reactive astrogliosis, and detection of virus either by quantitative RT-PCR for the number of copies of HIV RNA/mg tissue or by immuno-histochemical detection of the HIV capsid protein, p24 (DAKO, Carpenteria, CA, USA) (Langford et al. 2002).

Neurons and treatments

Mouse cortical neurons were obtained from C57BL mice, embryonic day 15 (E15) (Charles River Laboratories, Horsham, PA) by enzymatic and mechanical disruption. Temple University IACUC approved all studies. Briefly, intact brain tissue was placed into Hibernate medium (Brain Bits, Springfield, IL) and cortices were dissected. Following removal of meninges, cortical tissue was incubated in TrypleExpress enzyme (Invitrogen, Carlsbad, CA) at 37°C for 10 min. After washing in PBS, tissue trituration was conducted through a glass Pasteur pipette in Neurobasal medium containing B27 supplement, and 0.25 mM L-glutamine (Invitrogen). The resulting single cell suspension was diluted in culture medium and cells were plated on poly-D-lysine (100 ng/ml) (Sigma, St. Louis, MO) coated dishes at a density of approximately 2.5×10^5 per 60 mm dish. Cytosine β-D- arabino-furanoside hydrochloride (Ara C, (10 μM)) (Sigma) was added 24 h later to enrich for neurons by inhibiting cell proliferation. HIV Tat (cat # 2222) and gp120 (cat # 2968) proteins were obtained from the NIH AIDS Research and Reference Reagent Program. Neurons were exposed to Tat (100 nM), gp120 (25 ng/ml) or TNF-α (100 ng/ml) (Sigma) for varying lengths of time and then harvested for analyses.

Cell lines

The murine HT22 hippocampal medulloblastoma cell line, a subclone of HT4 (ATCC), was maintained in DMEM with 10% FBS and sodium pyruvate (Invitrogen). SHSY-5Y, a noradrenergic subclone of the SK-N-SY neuroblastoma cell line, was differentiated with 10 μm retinoic acid (Sigma) and cultured in Neurobasal medium with B-27 supplement and 200 nM glutamine (Invitrogen).

Double-labeling immunofluorescence and deconvolution microscopy

Paraffin-embedded frontal cortex tissues were processed, and immunohistochemistry was performed using the avidin–biotin–peroxidase methodology according to the manufacturer's instructions, with modifications (Vector Laboratories, Burlingame, CA, USA). Our modified protocol included de-paraffination in xylene, rehydration from alcohol to water, non-enzymatic antigen retrieval in citrate buffer, pH 6.0, for 1 h at 95°C, and quenching of endogenous peroxidase with 10% H_2O_2 in methanol for 20 min. After rinsing with 1× PBS, sections were blocked with normal goat serum for 1 h at room temperature and incubated overnight in a humidified chamber with rabbit polyclonal antibody against human PINCH (1:1,000) (Rearden et al. 2008). After rinsing three times with PBS, sections were incubated with a fluorescein isothiocyanate (FITC)-conjugated secondary antibody (1:500) for 2 h at room temperature in the dark. After washing with PBS, the sections were blocked with normal horse serum and incubated overnight at room temperature in a humidified chamber with mouse monoclonal primary antibodies for specific cellular markers including anti-SV2A (synaptic vesicle 2A) (1:100, Abcam, Cambridge, MA, USA) and anti-MAP2 (1:100, Covance, Emeryville, CA, USA). Sections were incubated with a rhodamine-tagged secondary antibody (1:500) for 2 h at room temperature in the dark.

Mouse primary neurons were plated at a density of 3×10^5/chamber in two-well glass chamber slides (Nunc, Rochester, NY, USA). After TNF-α treatment, slides were washed with PBS and fixed for 20 min at room temperature with 5% paraformaldehyde in PBS containing 0.02% Triton-X 20 min. After three 5-min washes in PBS, slides were blocked

with 5% BSA in PBS, and 0.02% Triton-X for 30 min, and incubated overnight at room temperature in a humidified chamber with anti-PINCH (1:500) (Rearden et al. 2008) or anti-ILK (1:250) antibodies (Santa Cruz Biotechnologies, Santa Cruz, CA, USA). The secondary antibodies used were FITC-conjugated anti-rabbit IgG (Vector) and rhodamine-conjugated anti-mouse IgG (Pierce) at 1:500 as describe above. All slides were mounted with an aqueous based media containing DAPI for nuclear labeling (Vectashield; Vector Laboratories) and visualized with a Nikon ultraviolet inverted microscope and processed with deconvolution software (Slidebook 4.0; Intelligent Imaging, Denver, CO, USA).

Western analyses

Nuclear and cytoplasmic extracts from cells were prepared using the Nuclear Extraction Kit (Pierce, Rockford, IL, USA), according to the manufacturer's instructions. For whole cell extract preparation, cells were lysed in 300 ml TNN buffer (50 mM Tris, 150 mM NaCl, and 0.5% NP-40 with protease inhibitor cocktail, Sigma). Cell debris was removed by centrifugation at 14,000 rpm for 15 min at 4°C. The protein concentration was measured by the Bradford assay, 35 mg lysate was loaded per well for SDS-PAGE, and proteins were transferred onto PVDF or nitrocellulose membranes. Western analyses were conducted by incubation with anti-PINCH (1:1,000, BD Biosciences, San Jose, CA, USA), anti-ILK (1:1,000, Santa Cruz Biotechnologies), anti-Nck2 (1:1,000, Santa Cruz Biotechnologies), and anti-Lamin A/C (1:1,000, Santa Cruz Biotechnologies) antibodies overnight at 4°C, followed by HRP-tagged secondary antibody (1:5,000, 1 h at room temperature, American Qualex, San Clemente, CA, USA). Anti-growth factor receptor bound protein (Grb2) (1:1,000) and anti-Tubulin antibodies (Cell Signaling Technologies, Danvers, MA, USA) were used as loading controls. Proteins were visualized by ECL (GE Healthsciences, Piscataway, NJ, USA), and densitometric calculations were conducted using ImageJ software (1.37v, NIH).

TNF-receptor neutralization

Neurons were treated with 10 μg/ml of neutralizing mouse anti-TNFR1 antibody (no. MAB225, R&D Systems) for 30 min (Hsiao et al. 2003) followed by TNF-α (100 ng/ml) for 72 h. Levels of PINCH were assessed by Western analyses as described above.

Immunoprecipitation

Proteins from nuclear and cytoplasmic cell lysates were prepared as described previously, and 500 mg was mixed with HNTG buffer (20 mM Hepes pH 7.5, 150 mM NaCl, 0.1% Triton-X100, 10% glycerol, and protease inhibitors) and 2.5 mg (10 μl) of anti-PINCH antibody (BD) to final volume 500 μl. After overnight incubation at 4°C rotating end over end, proteins were mixed with 20 μl of anti-mouse IgG-Agarose beads (Sigma) and incubated for 1.5 h. After washing, the beads with the precipitated proteins were released by boiling in SDS-PAGE sample buffer for 10 min. The samples were analyzed by Western blotting with anti-PINCH (1:1,000, BD) and ILK (1:1,000, Santa Cruz Biotechnologies) antibodies as described previously.

Antibody labeling and delivery

Eight milligrams of rabbit anti-PINCH antibody was labeled using the Chromeo 488 kit (Active Motif, Carlsbad, CA, USA) according to the manufacturer’s instructions. The labeled PINCH antibody was delivered into live neurons via the Chariot™ transfection reagent according to manufacturer’s instructions (Active Motif). Briefly, neurons were grown to approximately 70% confluence on chamber slides as described above. The Chariot™ reagent was incubated with 500 μl of 2 μg/μl of anti-PINCH antibody (Rearden et al. 2008) for 30 min at room temperature. The mixture was diluted 1:1 in serum free media,

overlaid onto neurons, and incubated for 2 h at 37°C at 5% CO_2. Neurons were then treated with TNF-alpha and were then fixed in cold acetone and processed for immunofluorescence labeling as described.

Neuronal fitness assays

Survival was determined by Trypan blue dye exclusion as previously described (Grigorian et al. 2008; Langford et al. 2004a). Briefly, 20 images were captured per condition, and a neurite was defined as a cellular process longer than the diameter of the cell body. Neurons with no processes longer than the cell body diameter were considered to have no processes. Neurite numbers and lengths were quantified with the aid of ImageJ 1.37v (Rasband 1997), and at least 150 neurons per condition were counted. The sum of the neurite number and of neurite length was divided by the number of cells counted, and the neurite length per cell was divided by the neurite number per cell, and defined as the average neurite length. Neurons with overlapping neurites or neurites that could not be clearly associated with a single neuron were not counted.

Statistics

Data were generated from at least three independent experiments. Statistical analyses were conducted using the Prism 4 GraphPad software program (GraphPad Software, Inc.). Data were analyzed by one-way ANOVA with Bonferroni's multiple comparison or Tukey–Kramer multiple post hoc where appropriate, and results were considered significant if $P \leq 0.05$.

Results

PINCH expression correlates with neurons showing decreased immunoreactivity for synaptodendritic markers

Our previous study showed that PINCH was expressed robustly by neurons in HIV infected patients' brains, but was undetectable in healthy controls (Rearden et al. 2008). Likewise, these studies showed that dystrophic neurons in the brains of HIV patients showed strong PINCH immunoreactivity, whereas adjacent neurons with normal morphology displayed much less PINCH immunoreactivity. Thus, to examine more closely selective neuronal expression of PINCH in the brains of HIV patients, we assessed expression levels of synaptodendritic markers in PINCH-reactive neurons from the brains of HIVE patients. PINCH immunoreactivity was increased in neurons showing a loss of either SVA2, an immunomarker for synaptic vesicles (Fig. 1a), or MAP2, a marker for dendritic arbor (Fig. 1b). Conversely, neurons with intense SVA2 or MAP2 labeling showed weak PINCH immunoreactivity. These results suggest that PINCH is expressed in the brains of HIV patients by neurons that also show a loss of synaptodendritic proteins.

PINCH levels increase in neurons exposed to TNF-α and Tat, but not gp120

These findings led us to investigate potential molecular mechanisms involved in PINCH induction. Numerous studies have shown that during HIV infection of the CNS and in in vivo and in vitro model systems, Tat and gp120, and the host inflammatory factor, TNF-α, contribute to neuronal dysfunction (Sabatier et al. 1991; Glowa et al. 1992; Magnuson et al. 1995; Nottet and Gendelman 1995; Janabi et al. 1998). To mimic some aspects of HIV-associated CNS disease in vitro, mouse primary neurons were exposed to Tat, gp120, and TNF-α. PINCH protein levels increased significantly in neurons exposed to Tat (approximately threefold, $p \leq 0.005$) and TNF-α (approximately fivefold, $p \leq 0.001$) treatment compared with un treated neurons (Fig. 2a, b). On the other hand, exposure to gp120 did not alter PINCH levels compared with untreated control (Fig. 2a, b). Since PINCH interacts

with ILK and Nck2 at focal adhesion junctions (Tu et al. 1998; Tu et al. 1999), we assessed ILK and Nck2 protein levels in neurons exposed to Tat and TNF-α. Both Tat and TNF-α increased ILK protein levels by approximately two- and fivefold, respectively ($p \leq 0.01$), whereas Nck2 levels were not affected (data not shown).

To address the specificity of TNF-α on changes in PINCH levels, mouse primary neurons were exposed to anti-TNF-receptor-1 neutralizing antibody followed by stimulation with TNF-α and assessed by Western analyses. Blocking the TNF receptor prior to stimulation with TNF-α greatly reduced PINCH levels (Fig. 2c), indicating that TNF-α induction of PINCH is mediated through the TNF receptor.

TNF-α induces changes in PINCH and ILK subcellular localization in neurons

Previous studies indicate that in response to injury, PINCH expression increases in Schwann cells and dorsal root ganglia neurons, and shuttles between the nucleus and cytoplasm (Campana et al. 2003). To assess the subcellular localization of PINCH and ILK, double immunofluorescence labeling of frontal cortex tissues from HIV patients' brains was conducted. Increased PINCH and ILK co-expression was observed clustering around the nuclei of neurons (Fig. 3a, b, arrowheads).

Next, we assessed in vitro whether changes in the subcellular distribution of PINCH accompanied increased protein levels of PINCH upon exposure to TNF-α. In control neurons, ILK (Fig. 3c, arrowheads, red) was organized in a pattern reminiscent of cytoskeletal elements, and PINCH (green) was distributed throughout the cytoplasm and the nucleus. Upon stimulation with TNF-α, the pattern of ILK subcellular localization changed dramatically and became distributed throughout the cell, with PINCH and ILK co-localizing in the perinuclear region of the neurons.

To further characterize these changes in subcellular distribution of PINCH and ILK, analyses of protein expression in nuclear and cytoplasmic fractions were conducted. In addition to TNF-α-induced increases in PINCH expression, other interesting patterns were observed in neurons exposed to TNF-α. First, significantly more PINCH protein was present in the nuclear fractions from both TNF-α stimulated *and* un-stimulated neurons (Fig. 4a, b). PINCH levels increased approximately twofold in the nuclear fraction and fourfold in the cytoplasmic fraction in TNF-α treated neurons compared with untreated neurons (Fig. 4b). Second, higher molecular weight immunoreactive bands of PINCH (~71- and 54-kDa) were prominent in the nuclear fraction. The higher molecular weight immunoreactive band (71-kDa) was not observed in the cytoplasmic fraction, although a faint band at 54-kDa was present (Fig. 4a, arrowhead). Detection of the ~71-kDa higher molecular weight band has been reported by our group and others and has been proposed to be the PINCH dimer (Campana et al. 2003; Rearden et al. 2008), although this has not been confirmed. Third, ILK protein from the nuclear fractions of TNF-α stimulated neurons was detected as a doublet (Fig. 4a). In this regard, ILK is reported to shuttle between the nucleus and cytoplasm, with the unphosphorylated protein accumulating in the nucleus (Acconcia et al. 2007). For quantitation, both bands in the doublet in the nuclear fraction of TNF-α treated neurons were analyzed and together account for the twofold increase in ILK observed in the nuclear fraction (Fig. 4c). No differences were observed in the cytoplasmic levels of ILK upon TNF-α treatment. These results suggest that upon exposure to TNF-α, not only do neuronal levels of PINCH and ILK increase, but subcellular localization is also altered. Detection of the cytoplasmic protein, α-tubulin, and the nuclear protein, Lamin A/C, confirmed fractionation fidelity (Fig. 4a).

To further address the 71-kDa molecular weight PINCH immunoreactive band and the ILK doublet observed in the nuclear fractions, we immunoprecipitated proteins from both nuclear

and cytoplasmic fractions with anti-PINCH antibody raised against a peptide spanning the third and fourth LIM domains of PINCH. Western analyses with anti-PINCH antibody revealed 100- and 37-kDa bands (Fig. 5a). The 71-kDa band was not visible, and the presence or absence of the 54-kDa band was obscured by the IgG heavy chain. Proteins immunoprecipitated with anti-PINCH antibody and detected by Western analysis with anti-ILK antibody revealed a doublet in the nuclear fraction at approximately 60-kDa (Figure 5b, arrowheads).

In the presence of TNF-α, antibody-mediated accumulation of PINCH protein results in fewer neurons with processes and in neurons with shorter processes

Since exposure to TNF-α alters cellular localization of PINCH and ILK, we disrupted PINCH protein intracellular mobility and subcellular localization to assess the effects on neuronal morphology. For this purpose, the Chariot™ system was utilized to deliver anti-PINCH antibody into live neurons (Morris et al. 2001; Remacle et al. 2005; Zhang et al. 2005). Control conditions included untreated and TNF-α-treated HT22 neurons, and neurons treated with Chariot™ without conjugated PINCH in the presence and absence of TNF-α. All control groups showed normal neuronal morphology consistent with untreated neurons with PINCH protein detected in the soma, processes, and nucleus (Fig. 6a, b). Anti-PINCH antibody complexed with Chariot™ was delivered into neurons in the presence (Fig. 6e, f) and absence (Fig. 6c, d) of TNF-α. Perinuclear accumulation of PINCH protein was observed in both cases (Fig. 6c, e), with little PINCH detected in processes or in the nucleus. Interestingly, in the absence of TNF-α treatment, PINCH sequestration had no effect on neurite extensions (Fig. 6b, c, d, arrowheads). On the other hand, when PINCH was sequestered followed by exposure to TNF-α, processes were retracted (Fig. 6e, f).

Sequestration of PINCH in the presence of TNF-α decreased the percentage of neurons with processes by approximately 80% (Fig. 6g). The lengths of existing processes were significantly shorter, as well, when compared with all other groups ($*p < 0.001$, Fig. 6h). These results suggest that PINCH protein mobility is required for extensions of neurites in response to TNF-α, whereas exposure to TNF-α without sequestration of PINCH protein has no effect on neuronal process extension.

Taken together, results from these studies suggest that TNF-α induces increased PINCH protein expression and alterations in its subcellular localization. Likewise, blocking the ability of PINCH to move throughout the neuron in the presence of TNF-α results in retraction of neurites. These findings show that upon stimulation with TNF-α, levels of neuronal PINCH protein increase and significant changes in its subcellular localization occur.

Discussion

In this study, we addressed the upregulation of PINCH protein in neurons in the brains of HIV patients by mimicking some aspects of HIV infection of the CNS. Pro-inflammatory cytokine production plays a particularly important role in vivo in HIV-associated dementia (HAD), and TNF-α is among the most consistently observed and markedly elevated cytokines in HAD. Produced by both infected and uninfected activated brain macrophages and microglia (Grimaldi et al. 1991; Achim et al. 1993; Wesselingh et al. 1993; Glass et al. 1995; Wesselingh et al. 1997; Adle-Biassette et al. 1999; Rostasy et al. 1999; Saha and Pahan 2003), TNF-α is functionally important, as it is believed to contribute to neuronal injury through direct and indirect mechanisms (Gelbard et al. 1993; Chao and Hu 1994; Fine et al. 1996; Bezzi et al. 2001). In one study, increased plasma levels of TNF-α levels were associated with shorter time to development of HAD (Sevigny et al. 2007). Many in vitro studies report that TNF-α and the HIV protein, Tat, are toxic to neurons in vitro (Theodore

et al. 2006; Buscemi et al. 2007), and increased levels of TNF-α correlate with severity of HIV dementia (Wesselingh et al. 1993). In addition to its role in neuropathogenesis, elevated TNF-α may contribute to immunopathogenesis and can upregulate viral replication (Aukrust et al. 1994; Chun et al. 1998).

We have shown that although Tat significantly increased PINCH expression in neurons, levels of TNF-α-induced PINCH expression were twofold greater than those of Tat-induced expression (Fig. 2). Considering the fact that Tat induces TNF-α production in neurons (Contreras et al. 2005;Buscemi et al. 2007), these results are not unexpected. Specifically, Tat activates the transcription of TNF-α (Buonaguro et al. 1992). On the other hand, exposure of neurons to gp120 failed to induce PINCH expression. Induction of TNF-α by gp120 in pure astrocytic cultures has been reported (Buriani et al. 1999). Likewise, gp120 is toxic to neurons indirectly by activation of microglia and astrocytes, which in turn release TNF-α (Lipton 1993;Nath 2002). If neurons were co-cultured with astrocytes, and exposed to gp120, it is possible that glial production of TNF-α may induce PINCH expression; however, this has not been shown. Although TNFR neutralizing antibodies partially blocked TNF-α-induced PINCH expression, other factors could contribute to PINCH expression as well. In this regard, upregulation of PINCH may be observed in other CNS diseases with inflammatory components. As a matter of fact, TNF-α levels in brain tissue, CSF, and plasma have been found to be elevated in several CNS disorders, including HIV infection (Merrill and Chen 1991). Our findings support that TNF-α released as a response to infection might trigger additional stress response genes or/and proteins, including PINCH.

Since an increase in PINCH protein was observed in neurons with decreased expression of markers for synaptodendritic complexity (Fig. 1), we reasoned that PINCH might be induced in neurons that are damaged and are attempting to recover or to prevent further injury. Moreover, PINCH may function as a survival signal as studies in other cell systems have shown that PINCH expression by tumor cells inhibits apoptosis via ERK-BIM signaling (Chen et al. 2008). Our findings that neurites retract upon challenge with TNF-α only when PINCH protein is sequestered (Fig. 6) points to a role for PINCH in neuronal attachment and spreading. Indeed, many studies show that without proper PINCH localization in the cell, migration and focal adhesion interactions with the extracellular matrix are disrupted (Tu et al. 1999;Dougherty et al. 2005;Li et al. 2005). Although we did not observe neuronal death upon PINCH sequestration and TNF-α stimulation, it is possible that apoptotic pathways may be induced in extended treatments.

Reorganization of PINCH and ILK in neurons upon exposure to TNF-α along with dramatic changes in cytoplasmic/nuclear distribution suggests functional roles for both proteins during TNF-α pathway stimulation. Regarding PINCH, previous studies described putative overlapping C-terminal nuclear localization and export signal sequences (Campana et al. 2003), but the potential roles of PINCH in the nucleus versus the cytoplasm have not been established. Interestingly, the ~72-kDa band detected in Fig. 4 is reminiscent of the findings reported by several groups (Jiang et al. 2010; Campana et al. 2003; Rearden et al. 2008) and may represent a PINCH dimmer, although all analyses were conducted under reducing conditions. In our hands, upon immunoprecipitation and Western analyses with anti-PINCH antibody, the higher molecular weight 71-kDa band was not detected. The 54-kDa band that we observed in the nuclear fractions of neurons (Fig. 4) has been shown in some other studies, but its identity was not discussed (Yang et al. 2005) (Chen et al. 2008). This form of PINCH may represent a degradation product of the 71-kDa band, or a modified and as yet unidentified form of PINCH.

On the other hand, the phosphorylation state of ILK has been reported as key in determining subcellular location. Acconcia et al. reported p21 activated kinase-1-mediated

phosphorylation of ILK and the presence of nuclear import and export motifs in the ILK sequence (Acconcia et al. 2007). ILK phosphorylation mutants failed to localize to the nucleus, suggesting that phosphorylation is key for ILK transport to the nucleus. These findings parallel with our observation of an ILK doublet exclusively in the nuclear fraction of neurons exposed to TNF-α (Fig. 4). As shown in Fig. 3c, ILK patterns in the cytoplasm reflect a “cytoskeletal-like” organization and may represent ILK complexed to a binding partner, although at this point no conclusive data exist to support this notion. Likewise, reasons for the apparent decreased PINCH–ILK co-localization in untreated neurons are unclear. Studies to elucidate whether the lower band of the doublet represents an unphosphorylated form of ILK are underway.

Taken together, these studies show that in neurons, PINCH and ILK localization and expression are regulated by TNF-α. Given that the HIV protein Tat, but not gp120, induced PINCH expression, it is quite possible that PINCH is increased in the neurons of other CNS diseases with inflammatory components. Based on studies that PINCH expression stabilizes some tumorogenic cells by averting the apoptosis pathway, it is feasible that PINCH is induced in neurons during HIV infection or other diseases as a survival signal or to initiate repair mechanisms.

Acknowledgments

This work was made possible by R01MH085602 to TDL. We acknowledge Dr. Ann Rearden for consultation and the HIV Neurobehavioral Research Center (HNRC) and the California NeuroAIDS Tissue Network (CNTN) for providing human brain tissues. The HNRC is supported by center award MH62512 and CNTN byMH059745.We thank Britt Tracy for assistance with manuscript preparation and editing.

References

1. Acconcia F, Barnes CJ, Singh RR, Talukder AH, Kumar R. Phosphorylation-dependent regulation of nuclear localization and functions of integrin-linked kinase. Proc Natl Acad Sci USA. 2007; 104:6782–6787. [PubMed: 17420447]
2. Achim CL, Heyes MP, Wiley CA. Quantitation of human immunodeficiency virus, immune activation factors, and quinolinic acid in AIDS brains. J Clin Invest. 1993; 91:2769–2775. [PubMed: 8514884]
3. Adle-Biassette H, Chretien F, Wingertsmann L, Hery C, Ereau T, Scaravilli F, Tardieu M, Gray F. Neuronal apoptosis does not correlate with dementia in HIV infection but is related to microglial activation and axonal damage. Neuropathol Appl Neurobiol. 1999; 25:123–133. [PubMed: 10216000]
4. Aukrust P, Liabakk NB, Muller F, Lien E, Espevik T, Froland SS. Serum levels of tumor necrosis factor-alpha (TNF alpha) and soluble TNF receptors in human immunodeficiency virus type 1 infection—correlations to clinical, immunologic, and virologic parameters. J Infect Dis. 1994; 169:420–424. [PubMed: 7906293]
5. Bansal AK, Mactutus CF, Nath A, Maragos W, Hauser KF, Booze RM. Neurotoxicity of HIV-1 proteins gp120 and Tat in the rat striatum. Brain Res. 2000; 879:42–49. [PubMed: 11011004]
6. Bezzi P, Domercq M, Brambilla L, Galli R, Schols D, De Clercq E, Vescovi A, Bagetta G, Kollias G, Meldolesi J, Volterra A. CXCR4-activated astrocyte glutamate release via TNFalpha: amplification by microglia triggers neurotoxicity. Nat Neurosci. 2001; 4:702–710. [PubMed: 11426226]
7. Buonaguro L, Barillari G, Chang HK, Bohan CA, Kao V, Morgan R, Gallo RC, Ensoli B. Effects of the human immunodeficiency virus type 1 Tat protein on the expression of inflammatory cytokines. J Virol. 1992; 66:7159–7167. [PubMed: 1279199]
8. Buriani A, Petrelli L, Facci L, Romano PG, Dal Tosso R, Leon A, Skaper SD. Human immunodeficiency virus type 1 envelope glycoprotein gp120 induces tumor necrosis factor-alpha in astrocytes. J NeuroAIDS. 1999; 2:1–13. [PubMed: 16873189]

9. Buscemi L, Ramonet D, Geiger JD. Human immunodeficiency virus type-1 protein Tat induces tumor necrosis factor-alpha-mediated neurotoxicity. Neurobiol Dis. 2007; 26:661–670. [PubMed: 17451964]
10. Campana WM, Myers RR, Rearden A. Identification of PINCH in Schwann cells and DRG neurons: shuttling and signaling after nerve injury. Glia. 2003; 41:213–223. [PubMed: 12528177]
11. Chao CC, Hu S. Tumor necrosis factor-alpha potentiates glutamate neurotoxicity in human fetal brain cell cultures. Dev Neurosci. 1994; 16:172–179. [PubMed: 7705222]
12. Chen K, Tu Y, Zhang Y, Blair HC, Zhang L, Wu C. PINCH-1 regulates the ERK-Bim pathway and contributes to apoptosis resistance in cancer cells. J Biol Chem. 2008; 283:2508–2517. [PubMed: 18063582]
13. Cherner M, Cysique L, Heaton RK, Marcotte TD, Ellis RJ, Masliah E, Grant I. Neuropathologic confirmation of definitional criteria for human immunodeficiency virus-associated neurocognitive disorders. J Neurovirol. 2007; 13:23–28. [PubMed: 17454445]
14. Chun TW, Engel D, Mizell SB, Ehler LA, Fauci AS. Induction of HIV-1 replication in latently infected CD4+ T cells using a combination of cytokines. J Exp Med. 1998; 188:83–91. [PubMed: 9653086]
15. Contreras X, Bennasser Y, Chazal N, Moreau M, Leclerc C, Tkaczuk J, Bahraoui E. Human immunodeficiency virus type 1 Tat protein induces an intracellular calcium increase in human monocytes that requires DHP receptors: involvement in TNF-alpha production. Virology. 2005; 332:316–328. [PubMed: 15661163]
16. Del Valle L, Pina-Oviedo S. HIV disorders of the brain: pathology and pathogenesis. Front Biosci. 2006; 11:718–732. [PubMed: 16146764]
17. Dougherty GW, Chopp T, Qi SM, Cutler ML. The Ras suppressor Rsu-1 binds to the LIM 5 domain of the adaptor protein PINCH1 and participates in adhesion-related functions. Exp Cell Res. 2005; 306:168–179. [PubMed: 15878342]
18. Ellis R, Langford D, Masliah E. HIV and antiretroviral therapy in the brain: neuronal injury and repair. Nat Rev Neurosci. 2007; 8:33–44. [PubMed: 17180161]
19. Fine SM, Angel RA, Perry SW, Epstein LG, Rothstein JD, Dewhurst S, Gelbard HA. Tumor necrosis factor alpha inhibits glutamate uptake by primary human astrocytes. Implications for pathogenesis of HIV-1 dementia. J Biol Chem. 1996; 271:15303–15306. [PubMed: 8663435]
20. Gelbard HA, Dzenko KA, DiLoreto D, del Cerro C, del Cerro M, Epstein LG. Neurotoxic effects of tumor necrosis factor alpha in primary human neuronal cultures are mediated by activation of the glutamate AMPA receptor subtype: implications for AIDS neuropathogenesis. Dev Neurosci. 1993; 15:417–422. [PubMed: 7835247]
21. Glass JD, Fedor H, Wesselingh SL, McArthur JC. Immunocytochemical quantitation of human immunodeficiency virus in the brain: correlations with dementia. Ann Neurol. 1995; 38:755–762. [PubMed: 7486867]
22. Glowa JR, Panlilio LV, Brenneman DE, Gozes I, Fridkin M, Hill JM. Learning impairment following intracerebral administration of the HIV envelope protein gp120 or a VIP antagonist. Brain Res. 1992; 570:49–53. [PubMed: 1617429]
23. Grigorian A, Hurford R, Chao Y, Patrick C, Langford TD. Alterations in the Notch4 pathway in cerebral endothelial cells by the HIV aspartyl protease inhibitor, nelfinavir. BMC Neurosci. 2008; 9:27. [PubMed: 18302767]
24. Grimaldi LM, Martino GV, Franciotta DM, Brustia R, Castagna A, Pristera R, Lazzarin A. Elevated alpha-tumor necrosis factor levels in spinal fluid from HIV-1-infected patients with central nervous system involvement. Ann Neurol. 1991; 29:21–25. [PubMed: 1996875]
25. Guo W, Jiang H, Gray V, Dedhar S, Rao Y. Role of the integrin-linked kinase (ILK) in determining neuronal polarity. Dev Biol. 2007; 306:457–468. [PubMed: 17490631]
26. Hsiao KC, Brissette RE, Wang P, Fletcher PW, Rodriguez V, Lennick M, Blume AJ, Goldstein NI. Peptides identify multiple hotspots within the ligand binding domain of the TNF receptor 2. Proteome Sci. 2003; 1:1. [PubMed: 12646066]
27. Janabi N, Di Stefano M, Wallon C, Hery C, Chiodi F, Tardieu M. Induction of human immunodeficiency virus type 1 replication in human glial cells after proinflammatory cytokines

stimulation: effect of IFNgamma, IL1beta, and TNFalpha on differentiation and chemokine production in glial cells. Glia. 1998; 23:304–315. [PubMed: 9671961]

28. Jiang Y, Mizisin AP, Rearden A, Jolivalt CG. Diabetes induces changes in ILK, PINCH and components of related pathways in the spinal cord of rats. Brain Res. 2010; 1332:100–109. [PubMed: 20347724]
29. Kim HJ, Martemyanov KA, Thayer SA. Human immunodeficiency virus protein Tat induces synapse loss via a reversible process that is distinct from cell death. J Neurosci. 2008; 28:12604–12613. [PubMed: 19036954]
30. Langford D, Sanders VJ, Mallory M, Kaul M, Masliah E. Expression of stromal cell-derived factor 1alpha protein in HIV encephalitis. J Neuroimmunol. 2002; 127:115–126. [PubMed: 12044982]
31. Langford D, Grigorian A, Hurford R, Adame A, Crews L, Masliah E. The role of mitochondrial alterations in the combined toxic effects of human immunodeficiency virus Tat protein and methamphetamine on calbindin positive-neurons. J Neurovirol. 2004a; 10:327–337. [PubMed: 15765804]
32. Langford D, Grigorian A, Hurford R, Adame A, Ellis RJ, Hansen L, Masliah E. Altered P-glycoprotein expression in AIDS patients with HIV encephalitis. J Neuropathol Exp Neurol. 2004b; 63:1038–1047. [PubMed: 15535131]
33. Li F, Zhang Y, Wu C. Integrin-linked kinase is localized to cell–matrix focal adhesions but not cell-cell adhesion sites and the focal adhesion localization of integrin-linked kinase is regulated by the PINCH-binding ANK repeats. J Cell Sci. 1999; 112(Pt 24):4589–4599. [PubMed: 10574708]
34. Li S, Bordoy R, Stanchi F, Moser M, Braun A, Kudlacek O, Wewer UM, Yurchenco PD, Fassler R. PINCH1 regulates cell–matrix and cell-cell adhesions, cell polarity and cell survival during the peri-implantation stage. J Cell Sci. 2005; 118:2913–2921. [PubMed: 15976450]
35. Lipton SA. Human immunodeficiency virus-infected macrophages, gp120, and N-methyl-D-aspartate receptor-mediated neurotoxicity. Ann Neurol. 1993; 33:227–228. [PubMed: 8434889]
36. Magnuson DS, Knudsen BE, Geiger JD, Brownstone RM, Nath A. Human immunodeficiency virus type 1 Tat activates non-N-methyl-D-aspartate excitatory amino acid receptors and causes neurotoxicity. Ann Neurol. 1995; 37:373–380. [PubMed: 7695237]
37. Merrill JE, Chen IS. HIV-1, macrophages, glial cells, and cytokines in AIDS nervous system disease. FASEB J. 1991; 5:2391–2397. [PubMed: 2065887]
38. Morris MC, Depollier J, Mery J, Heitz F, Divita G. A peptide carrier for the delivery of biologically active proteins into mammalian cells. Nat Biotechnol. 2001; 19:1173–1176. [PubMed: 11731788]
39. Nath A. Human immunodeficiency virus (HIV) proteins in neuropathogenesis of HIV dementia. J Infect Dis. 2002; 186 Suppl 2:S193–S198. [PubMed: 12424697]
40. Nottet HS, Gendelman HE. Unraveling the neuroimmune mechanisms for the HIV-1-associated cognitive/motor complex. Immunol Today. 1995; 16:441–448. [PubMed: 7546209]
41. Rasband, WS. ImageJ. 1.37 editionBethesda: NIH; 1997.
42. Rearden A. A new LIM protein containing an autoepitope homologous to “senescent cell antigen”. Biochem Biophys Res Commun. 1994; 201:1124–1131. [PubMed: 7517666]
43. Rearden A, Hurford RG, Luu N, Kieu E, Sandoval M, Perez-Liz G, Del Valle L, Powell H, Langford TD. Novel expression of PINCH in the CNS and its potential as a biomarker for HIV-associated neurodegeneration. J Neurosci Res. 2008; 86:2535–2542. [PubMed: 18459134]
44. Remacle AG, Rozanov DV, Baciu PC, Chekanov AV, Golubkov VS, Strongin AY. The transmembrane domain is essential for the microtubular trafficking of membrane type-1 matrix metalloproteinase (MT1-MMP). J Cell Sci. 2005; 118:4975–4984. [PubMed: 16219679]
45. Rostasy K, Monti L, Yiannoutsos C, Kneissl M, Bell J, Kemper TL, Hedreen JC, Navia BA. Human immunodeficiency virus infection, inducible nitric oxide synthase expression, and microglial activation: pathogenetic relationship to the acquired immunodeficiency syndrome dementia complex. Ann Neurol. 1999; 46:207–216. [PubMed: 10443886]
46. Sabatier JM, Vives E, Mabrouk K, Benjouad A, Rochat H, Duval A, Hue B, Bahraoui E. Evidence for neurotoxic activity of tat from human immunodeficiency virus type 1. J Virol. 1991; 65:961–967. [PubMed: 1898974]

47. Saha RN, Pahan K. Tumor necrosis factor-alpha at the crossroads of neuronal life and death during HIV-associated dementia. J Neurochem. 2003; 86:1057–1071. [PubMed: 12911614]
48. Sevigny JJ, Albert SM, McDermott MP, Schifitto G, McArthur JC, Sacktor N, Conant K, Selnes OA, Stern Y, McClernon DR, Palumbo D, Kieburtz K, Riggs G, Cohen B, Marder K, Epstein LG. An evaluation of neurocognitive status and markers of immune activation as predictors of time to death in advanced HIV infection. Arch Neurol. 2007; 64:97–102. [PubMed: 17210815]
49. Theodore S, Cass WA, Nath A, Steiner J, Young K, Maragos WF. Inhibition of tumor necrosis factor-alpha signaling prevents human immunodeficiency virus-1 protein Tat and methamphetamine interaction. Neurobiol Dis. 2006; 23:663–668. [PubMed: 16828290]
50. Tu Y, Li F, Wu C. Nck-2, a novel Src homology2/3-containing adaptor protein that interacts with the LIM-only protein PINCH and components of growth factor receptor kinase-signaling pathways. Mol Biol Cell. 1998; 9:3367–3382. [PubMed: 9843575]
51. Tu Y, Li F, Goicoechea S, Wu C. The LIM-only protein PINCH directly interacts with integrin-linked kinase and is recruited to integrin-rich sites in spreading cells. Mol Cell Biol. 1999; 19:2425–2434. [PubMed: 10022929]
52. Wesselingh SL, Takahashi K, Glass JD, McArthur JC, Griffin JW, Griffin DE. Cellular localization of tumor necrosis factor mRNA in neurological tissue from HIV-infected patients by combined reverse transcriptase/polymerase chain reaction in situ hybridization and immunohistochemistry. J Neuroimmunol. 1997; 74:1–8. [PubMed: 9119960]
53. Wesselingh SL, Power C, Glass JD, Tyor WR, McArthur JC, Farber JM, Griffin JW, Griffin DE. Intracerebral cytokine messenger RNA expression in acquired immunodeficiency syndrome dementia. Ann Neurol. 1993; 33:576–582. [PubMed: 8498837]
54. Wu C. Integrin-linked kinase and PINCH: partners in regulation of cell–extracellular matrix interaction and signal transduction. J Cell Sci. 1999; 112(Pt 24):4485–4489. [PubMed: 10574698]
55. Wu C. The PINCH–ILK–parvin complexes: assembly, functions and regulation. Biochim Biophys Acta. 2004; 1692:55–62. [PubMed: 15246679]
56. Yang Y, Guo L, Blattner SM, Mundel P, Kretzler M, Wu C. Formation and phosphorylation of the PINCH-1-integrin linked kinase-alpha-parvin complex are important for regulation of renal glomerular podocyte adhesion, architecture, and survival. J Am Soc Nephrol. 2005; 16:1966–1976. [PubMed: 15872073]
57. Yao H, Allen JE, Zhu X, Callen S, Buch S. Cocaine and human immunodeficiency virus type 1 gp120 mediate neurotoxicity through overlapping signaling pathways. J Neurovirol. 2009; 15:164–175. [PubMed: 19319745]
58. Zhang Q, Nottke A, Goodman RH. Homeodomain-interacting protein kinase-2 mediates CtBP phosphorylation and degradation in UV-triggered apoptosis. Proc Natl Acad Sci USA. 2005; 102:2802–2807. [PubMed: 15708980]

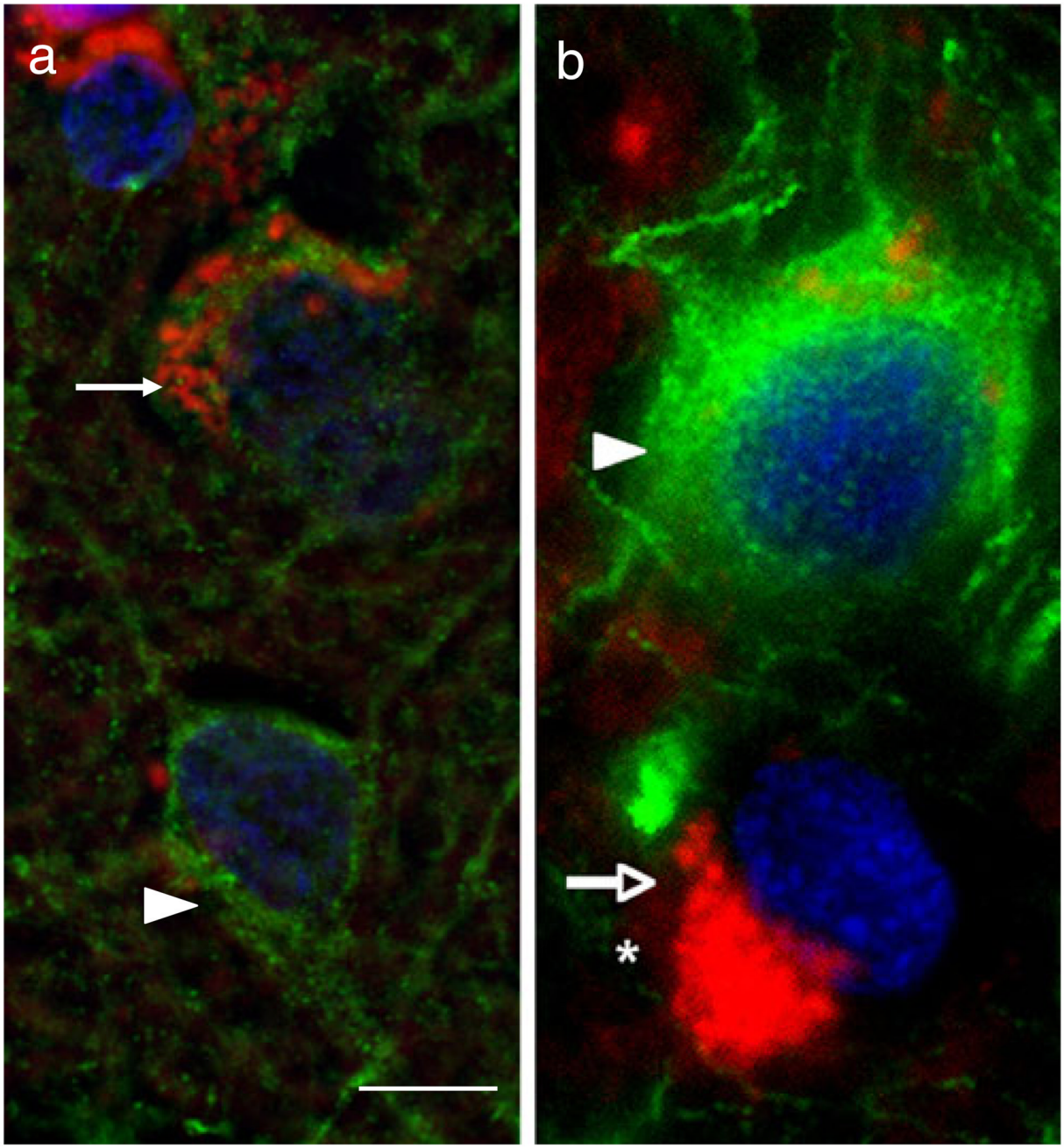

Fig. 1. PINCH expression by neurons in the human frontal cortex of an HIVE patient correlates with loss of synaptic vesicles and dendrites

a Double immunolabeling with anti-PINCH antibody (*red*) and anti-SV2A antibody specific for synaptic vesicles (*green*) shows abundant peri-nuclear PINCH immunoreactivity (*arrow*) in a neuron with decreased SV2A, indicating loss of synaptic vesicles. Compare with the adjacent neuron with well-preserved synapses (*arrowhead*) and no PINCH immunoreactivity. **b** Double immunolabeling with anti-PINCH antibody (*red*) and anti-MAP2 antibody (*green*) showing abundant peri-nuclear PINCH immunoreactivity (*arrow, red*) of a neuron with decreased dendritic complexity (*asterisk*). Compare with the adjacent

neuron with well-preserved dendritic complexity (*arrowhead, green*) and no PINCH immunoreactivity. Nuclei are labeled with DAPI (*blue*). *Scale bar* = 10 μm

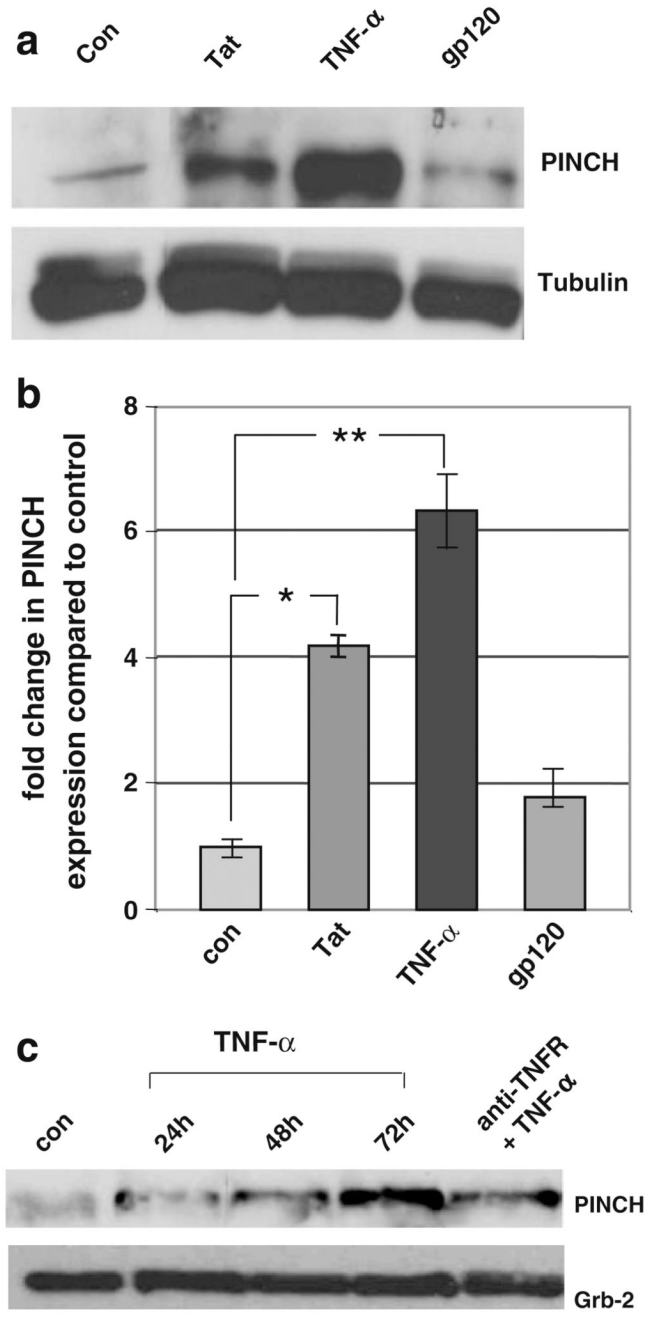

Fig. 2. Exposure to TNF-α and Tat, but not gp120, increases PINCH expression in mouse primary neurons

a Representative Western blot of untreated (C*on*), neurons exposed to 100 nM full length Tat, 100 ng/ml TNFα, or 25 nM gp120 for 72 h and reacted with anti-PINCH antibody. **b** Upon exposure to Tat or TNF-α, PINCH protein levels increased significantly above untreated control (**p*<0.005, ***p*<0.001, respectively, by one-way ANOVA with Bonferroni's multiple comparison). gp120 showed insignificant changes in PINCH protein compared with control. Graphed data represents three independent experiments. **c** PINCH levels in mouse primary neurons treated for 24, 48, or 72 h with TNF-α or with TNF-receptor neutralizing antibody (*TNFR*) for 30 min followed by TNF-α for 72 h

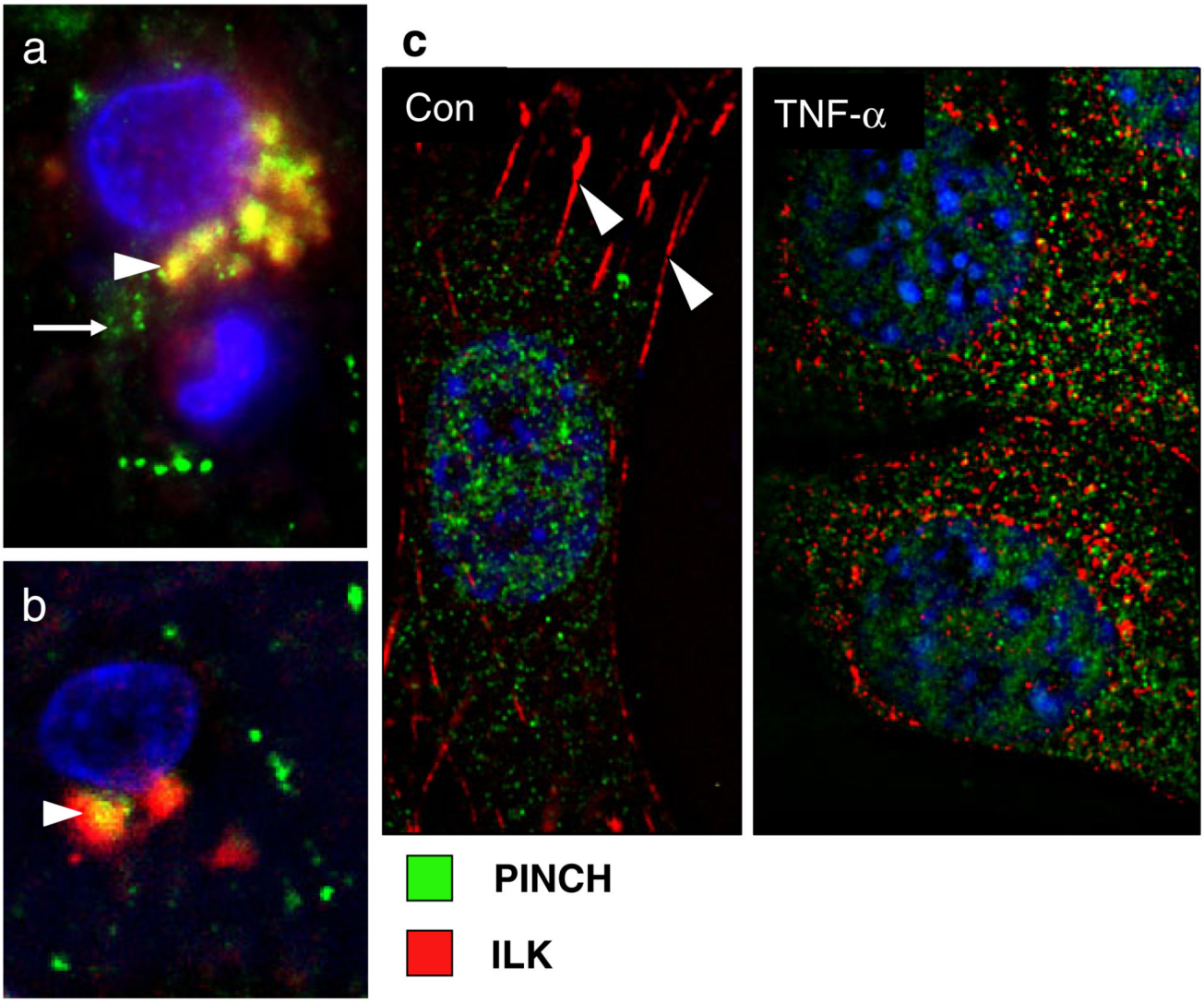

Fig. 3. PINCH/ILK co-expression in neurons increases in HIVE and upon TNF-α treatment

a, b Double immunofluorescent labeling of PINCH (*green, arrow*) and ILK (*red*) in frontal cortex from HIVE patients showing colocalization of perinuclear PINCH and ILK (*arrowheads*). **c** Untreated (*Con*) and TNF-α treated (72 h) neurons in vitro immunolabeled for PINCH (*green*) and ILK (*red, arrowheads*). Nuclei are labeled with DAPI (*blue*). Magnification, ×100

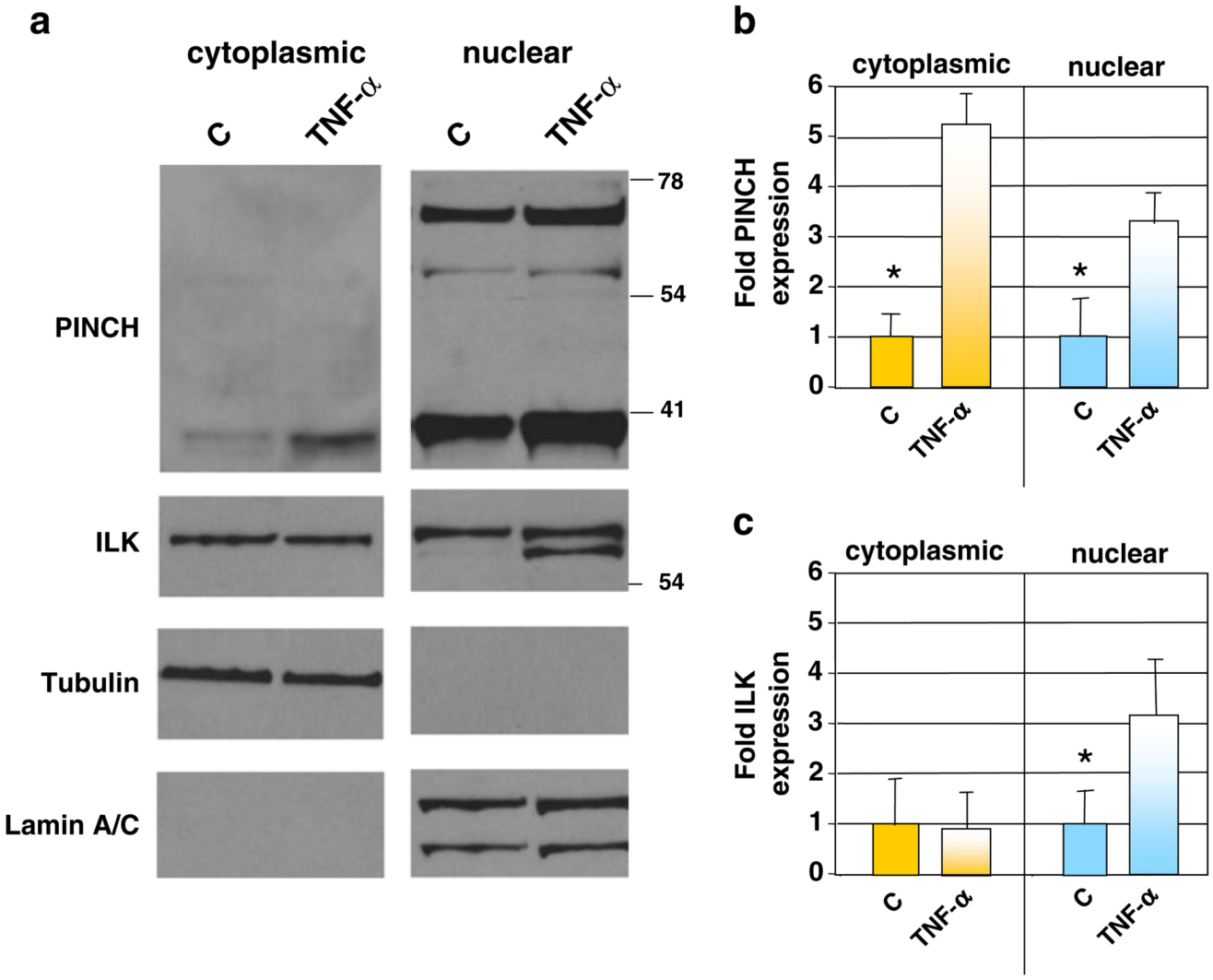

Fig. 4. TNF-α induced changes in PINCH and ILK localization

a Representative Western blot of PINCH and ILK in nuclear/cytoplasmic fractionation of mouse primary neurons±TNF-α. Tubulin and Lamin A/C were used as loading controls for cytoplasmic and nuclear fractions, respectively. The same blot was stripped and re-probed with each antibody shown. **b, c** Graphic representation of combined results from Western analyses showing fold changes in PINCH and ILK expression in both the cytoplasm and nucleus in untreated (*C*) and TNF-α treated neurons, $n=3$, $*p \leq 0.05$, by one-way ANOVA

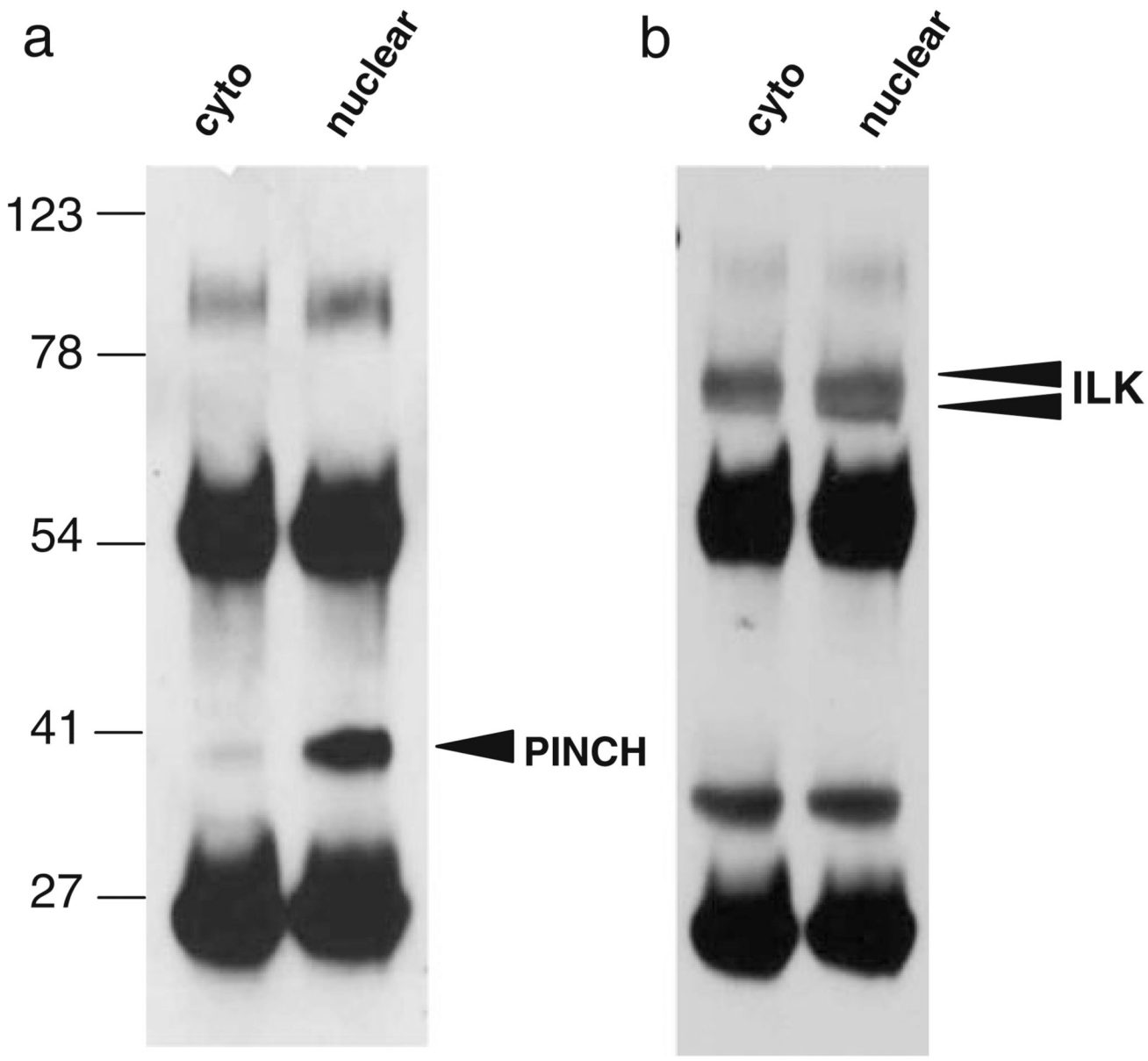

Fig. 5. Immunoprecipitation with anti-PINCH antibody confirms greater levels of PINCH in the nucleus and a nuclear ILK doublet

a Immunoprecipitation and Western analyses with anti-PINCH antibody reveal greater nuclear levels of PINCH at 37-kDa (*arrowhead*) compared with cytoplasmic. **b** Immunoprecipitation with anti-PINCH antibody and Western analyses with anti-ILK antibody reveals an ILK doublet in the nucleus at approximately 60-kDa (*arrowheads*)

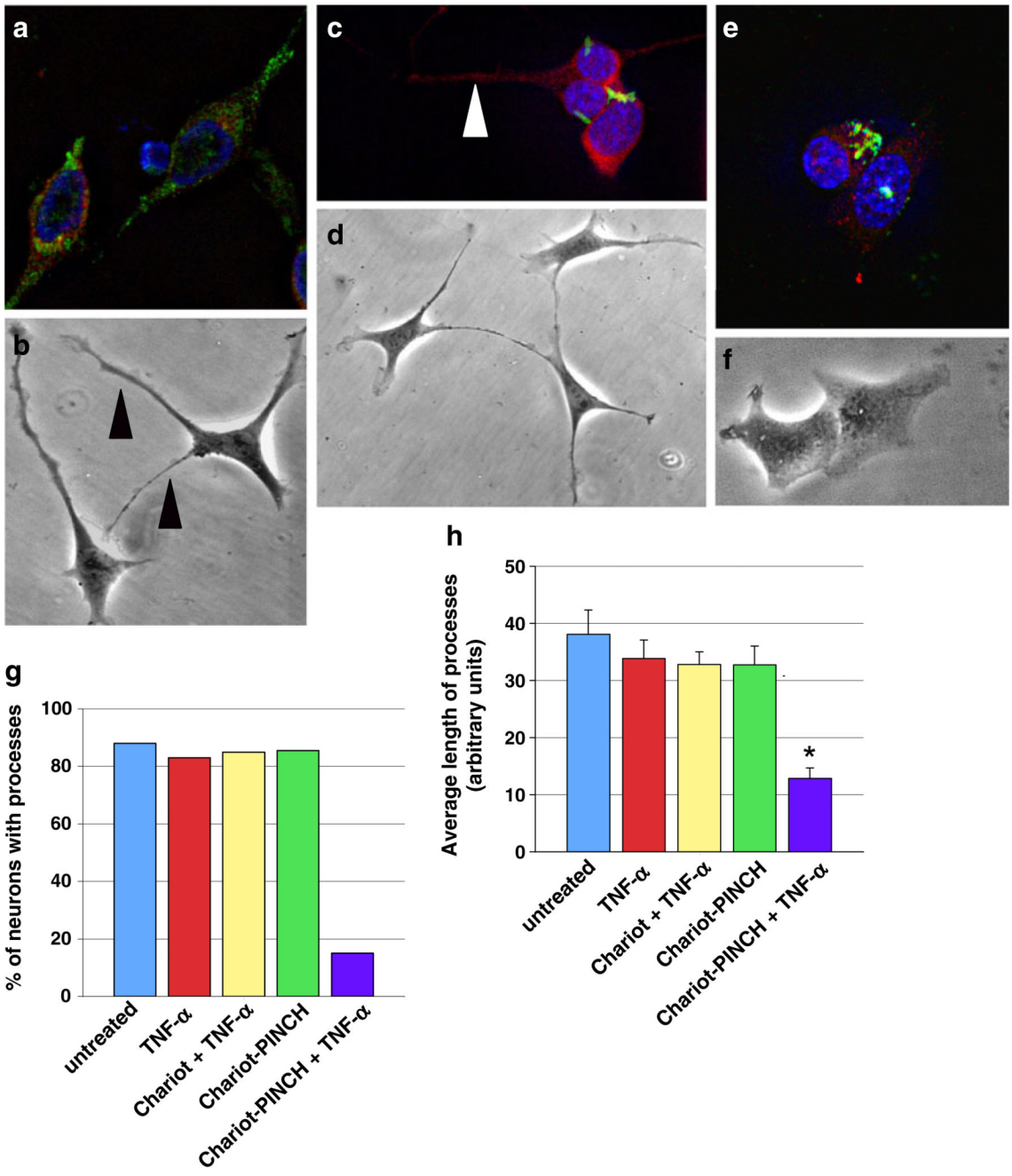

Fig. 6. Chariot-mediated delivery of anti-PINCH antibody into live neurons results in perinuclear accumulation of PINCH and retraction of processes upon exposure to TNF-α

a, c, e Representative HT22 neurons from treatment conditions labeled with anti-PINCH (*green*), anti-MAP2 (*red*), and nuclei with DAPI (*blue*). **b, d, f** Phase contrast images of HT22 neurons from each treatment condition. **a, b** Chariot without conjugated anti-PINCH antibody was delivered into live neurons followed by 48-h exposure to TNF-α. **c, d** Chariot-mediated delivery of anti-PINCH antibody in the absence of TNF-α. **e, f** Chariot-mediated delivery of anti-PINCH antibody followed by 48-h TNF-α treatment. **g** Percentage of neurons with processes, and **h**, average lengths of processes from untreated, TNF-α treated, Chariot delivered without anti-PINCH antibody conjugated followed by 48-h TNF-α

treatment (Chariot+TNF-α), Chariot-mediated delivery of anti-PINCH antibody in the absence of TNF-α (Chariot-PINCH), and Chariot-mediated delivery of anti-PINCH antibody followed by 48-h TNF-α treatment (Chariot-PINCH+TNF-α). Results from at least three independent experiments are expressed as percentage±SEM. *$p<0.001$ by one-way ANOVA with Tukey–Kramer multiple post hoc